J. Physiol. (1976), **262**, *pp.* 533–552
With 7 text-figures
Printed in Great Britain

INTRACELLULAR pH OF SINGLE CRUSTACEAN MUSCLE FIBRES BY THE DMO AND ELECTRODE METHODS DURING ACID AND ALKALINE CONDITIONS

BY J. A. M. HINKE AND M. R. MENARD

From the Department of Anatomy, University of British Columbia, Vancouver, B.C., V6T 1W5 Canada

(*Received 20 October 1975*)

SUMMARY

1. The intracellular pH of intact single muscle fibres of the giant barnacle was measured directly with a glass micro-electrode following prolonged (2–5 hr) equilibration in one of three solutions: normal Ringer, CO_2 Ringer and NH_4^+ Ringer.

2. The intracellular pH of identically-prepared fibres from the same specimen was measured indirectly from the distribution of DMO following prolonged equilibration in the same solutions.

3. The DMO-pH compared favourably with the electrode-pH_i provided DMO-pH_i was calculated from the values of the indicator compounds, [^{14}C]DMO and [^{3}H]inulin, obtained by extrapolating the slow uptake phase to time zero.

4. Following prolonged equilibration, the transmembrane H^+ ion distribution was found to vary with the membrane potential but not in accordance with a simple Gibbs–Donnan equilibrium.

5. A model which recognizes the existence of two independent net fluxes for H^+ across the membrane is developed to explain the results. One of the fluxes represents passive diffusion and the other represents the so called H^+-pump. The model predicts the H^+-pump rate increases by two orders of magnitude when pH_i is reduced from 7·2 to 6·7.

INTRODUCTION

It has often been observed on a variety of cells that the electrochemical potential of the H^+ ion is lower inside than it is outside the cell under resting conditions (Waddell & Bates, 1969). Since the cell membrane is quite permeable to the H^+ ion (Woodbury, 1971; Izutsu, 1972), one must seriously consider the existence of an outward-directed transport mechanism for the H^+ ion in order to explain how intracellular free H^+ can be

maintained at such a relatively low value, especially when one also considers that new H^+ ions can be generated from metabolic reactions. Unfortunately, the so-called 'proton pump' cannot be demonstrated by the conventional method of examining the unidirectional efflux of a H^+ isotope through the cell membrane.

Before becoming too committed to the existence of a 'proton pump', however, one should be reasonably satisfied that the intracellular pH measured experimentally adequately reflects the actual pH in the cytoplasm and does not contain a methodological error. Of the several methods employed or proposed for measuring intracellular pH (Waddell & Bates, 1969; Rose, 1968; Moon & Richards, 1973), the two which are considered most reliable are the weak electrolyte distribution method to give an indirect measure of cytoplasmic pH and impalement of the cell with a pH-glass micro-electrode to give a direct measure of cytoplasmic pH. In the former category, the weak acid, 5,5-dimethyloxazolidine-2,4-dione (DMO), is now most frequently used. Use of the pH micro-electrode is probably the method of choice but only a few laboratories have made use of it (Caldwell, 1954, 1958; Kostyuk & Sorokina, 1961; Carter, Rector, Campion & Seldin, 1967; McLaughlin & Hinke, 1968; Paillard, 1972; Thomas 1974; Aickin & Thomas, 1975) mainly because of the technical difficulty in constructing such electrodes with small enough tips for most cellular systems.

In a search of the literature over a year ago, we were surprised to find that no one had combined the DMO method with the pH micro-electrode in order to compare the two pH values in the same cell. We are here reporting on the results of such a study on single fibres of the giant barnacle, *Balanus nubilus*, but note that Boron & Roos (1976) have also completed a similar study on the same muscle preparation. Our results are comparable to but by no means identical with theirs.

This report also contains evidence that the transmembrane H^+ ion gradient is related to the resting potential after prolonged equilibration (> 2 hr) in both acid and alkaline Ringer solutions. This information is used to demonstrate the existence of a H^+ flux mechanism, in addition to the passive H^+ flux, which can adjust to the proton load. Some of this work has already appeared in abstract form (Menard, Nee & Hinke, 1975; Menard & Hinke, 1976).

METHODS

Tissue preparation. Barnacles were obtained from Puget Sound and maintained up to 3 months in artificial sea water at 10–12° C. Single fibres of the depressor scutorum lateralis or rostralis muscles were dissected free of each other but left attached in a bundle to the base plate, as previously described (McLaughlin & Hinke, 1966). The thin outer fibres of the depressor scutorum lateralis were always

discarded (Hoyle, McNeil & Selverston, 1973). Two such bundles from a given barnacle were incubated together for 2 hr in one of three solutions at 23·5° C before the start of an experiment: normal barnacle Ringer solution (in mM), Na^+, 450, K^+, 8; Ca^{2+}, 20; Mg^{2+}, 10; Cl^-, 518; Tris (hydroxymethyl) aminomethane, 25; pH ≐ 7·6; CO_2 Ringer solution (normal Ringer plus 1 mM-$NaHCO_3$ and continuous bubbling with 95% O_2 − 5%CO_2 gas mixture at a constant rate, pH ≐ 6·2); NH_4^+ Ringer solution (normal Ringer plus 5 mM-$(NH_4)_2SO_4$, pH ≐ 8·2). One bundle was used for micro-electrode measurements and one for a DMO uptake experiment. At the start of a DMO experiment, the bathing solutions were altered only by the addition of radio-isotopes.

DMO experiment. The base plate of the muscle bundle was anchored to a glass bar and the short tendon of each fibre was anchored to another glass bar by means of silk threads during incubation. The fibres were more or less parallel to one another and approximately at their *in situ* length. This assembly was then immersed in a continuously stirred 100 ml. bath of Ringer solution (one of the above) to which was added [^{14}C]DMO (to 300 disintegrations per minute (d.p.m.)/μl., SA = 8·8 mc/m-mole) and either [^{3}H]inulin (to 1000 d.p.m./μl., S.A. = 122 mc/g) or [^{3}H]sorbitol (to 1000 d.p.m./μl., S.A. = 200 mc/m-mole). At various times over the next three hours, single fibres were cut away from the assembly, rinsed for 30 sec in a zero-Na^+-sucrose solution isotonic with Ringer (McLaughlin & Hinke, 1966), blotted on filter paper and placed in pre-weighed stoppered liquid scintillation vials. After recording the wet weight and constant dry weight, the amounts of ^{14}C and ^{3}H isotopes in each fibre were determined on two channels of the Mark II Liquid Scintillation Counting System (Nuclear-Chicago, Searle). A manually adjustable window was used for the ^{3}H channel and a pre-set double-label window was used for the ^{14}C channel to maximize single channel counting efficiency and to minimize channels overlap. Efficiencies were determined by the external standards ratio method. The sixteen quenched standards (Amersham-Searle) contained ^{3}H or ^{14}C dissolved in the same scintillation medium as the unknown samples. Every sample was counted for at least 20 min and all sample counts were stable. Some fibres were wet ashed and analysed for Na^+ and K^+ content by flame photometry to check on the physiological state of the fibres. The bath was routinely analysed for ^{14}C, ^{3}H, [Na] and [K] at the beginning and end of each experiment. The pH of the bath was monitored continuously using commercial electrodes and a conventional pH meter.

Waddell & Butler (1959) made use of the following eqn. (1) in order to calculate intracellular pH, pH(DMO), from a DMO distribution experiment:

$$\text{pH (DMO)} = pK' + \log_{10}\left\{\left[\frac{C_t}{C_e}\left(1+\frac{V_e}{V_i}\right)-\frac{V_e}{V_i}\right][10^{(pH_e-pK')}+1]-1\right\}, \quad (1)$$

where K' is the empirical dissociation constant of DMO,
pH_e is the pH of the bath,
V_t is the analysed fibre water,
V_e is the extracellular water of the fibre,
$V_i = V_t - V_e$,
$C_e = [HDMO]_e + [DMO^-]_e$, total extracellular [^{14}C]DMO of fibre,
$C_t = ([HDMO]_i + [DMO^-]_i)\, V_i + C_e V_e]/V_t$, total [^{14}C]DMO of fibre.

In order to program a calculator to calculate pH (DMO) from the experimental data, eqn. (1) was rearranged as follows:

$$\text{pH (DMO)} = pK' + \log_{10}\left\{\left(\frac{[B_H]\,V_t}{D_H}-1\right)^{-1}\left(\frac{[B_H]\,D_C}{[B_C]\,D_H}-1\right)(10^{(pH_e-pK')}+1)-1\right\}, \quad (2)$$

where $[B_H]$ = $[[^3H]$inulin$]_e$ or $[[^3H]$sorbitol$]_e$ in d.p.m./unit bath volume
$[B_C]$ = $[[^{14}C]$ DMO$]_e$ in d.p.m./unit bath volume,
D_H is total ^3H (d.p.m.) in a blotted fibre, and
D_C is total ^{14}C (d.p.m.) in a blotted fibre

The [^{14}C]DMO, [^{3}H]inulin and [^{3}H]sorbitol isotopes were obtained from New England Nuclear at specific activities stated above. Non-radioactive DMO was obtained from Eastman Organic Chemicals. This was used to determine a pK' value for DMO at 23·5° C and in the presence of half-molar NaCl, corresponding to the uptake experiment. NaOH (CO_2-free) was used to titrate the acid form of DMO at two concentrations (0·5 and 1·0 mM), both in the absence and presence of 0·573 M-NaCl. The NaOH (CO_2-free) was obtained by treating a freshly prepared AgOH precipitate with a purged NaCl solution; the final concentration was tested by titration of potassium hydrogen phthalate. The conductimetric end point of the DMO–NaOH titration in the absence of NaCl was determined first and then the titration curve for the same volume of solution, containing the same amount of DMO, plus NaCl to 0·573 M was obtained, using a Radiometer Titrigraph. The resulting mean pK' values are 6·170 (S.D. of an observation = 0·032, n = 4) in the presence of 0·573 M-NaCl and 6·442 (S.D. of an observation = 0·051, n = 4) in the absence of NaCl. The former value was used in eqn. (2) for all pH (DMO) calculations. For comparison, Boron & Roos (1976) give a pK' value of 6·18 at 25° C for DMO in barnacle sea water and a pK' value of 6·33 at 25 °C for DMO in water.

pH micro-electrode experiment. The spear-type pH glass micro-electrodes were constructed from Corning 0150 glass, as previously described (Hinke, 1969). The outside diameter of the insulating glass at the seal to the sensitive glass was approximately 21μ. Each pH micro-electrode was routinely calibrated in standard buffer solutions immediately before and after a muscle fibre impalement. If the two calibration curves were significantly different the experiment was discarded. The calibration curves spanned the pH range from 4 to 9 and always had a slope of 58 mV/pH unit. Since the standard buffers made by us according to Robinson (1967) agreed exactly with commercially made buffer solutions the two sets were combined to give five calibration points over the pH range. Standard 3·5 M-KCl-filled micropipettes were drawn from Corning 0120 lead glass tubing to open tips of less than 1 μm diameter. A micropipette was selected for an experiment if its potential, relative to a standard calomel electrode, changed by less than 3 mV when the solution was changed from 0·2 M-KCl to 0·2 M-NaCl.

The method of McLaughlin & Hinke (1966) for electrode impalement of a single fibre was adopted. Briefly, the tendon of a fibre was cannulated without damaging the sarcolemma and then the fibre was suspended vertically in a bathing solution. The pH micro-electrode was passed down the cannula and advanced more than 1 cm into the myoplasm along the fibre's long central axis. As soon as advancement of the pH micro-electrode was stopped, the puncture wound in the sarcolemma at the tendon usually 'healed' within seconds, making retraction of the pH micro-electrode difficult. Adequate electrical as well as physical sealing (McLaughlin & Hinke, 1966) was checked by measuring the members potential (E_m) with the micropipette at 0·5, 1·0 and 2·0 cm distal to the puncture site. In all positions, the membrane potential was similar in magnitude. Finally, the micropipette was positioned in the myoplasm close to the tip of the pH micro-electrode.

The bath contained a standard calomel electrode which was connected to earth through a precision potentiometer which was routinely calibrated by a standard Weston cell. Depending on the availability of equipment, the pH micro-electrode and micropipette potentials (with reference to the calomel electrode) were measured alternately on a Keithley 616 electrometer or were measured simultaneously, one on a Cary 401 vibrating-reed electrometer and the other on the Keithley 616

electrometer. The electrometer output was reduced to zero by means of the precision potentiometer, then followed on a chart recorder in order to monitor electrode drift at a high sensitivity setting. In some experiments, the pH microelectrode was referred first to the bath calomel electrode and then to the indwelling micropipette. Obviously, the difference between the two observed potentials must equal the membrane potential and in all cases this was found to be so within ± 1 mV. In our experience, both the pH micro-electrode and the micropipette behaved best when they were referred to the bath calomel electrode, when the calomel electrode was earthed and when the electrometer output was made to read close to zero.

At the end of each measurement, the impaled fibre together with a companion fibre was removed for Na^+, K^+ and water analysis. The electrolyte and water contents of the impaled and non-impaled fibres were not significantly different. Furthermore, their mean values (not corrected for the extracellular space) were not different from the mean values of fibres used in the DMO experiments (Table 2).

If an impaled fibre showed any sign of damage the data from it was discarded. Damage to a single fibre cannot always be detected during dissection but can always be detected after 2 hr of incubation. An undamaged fibre is uniformly translucent, remains at its *in situ* length and displays a constant diameter throughout its length. A damaged fibre reveals itself by a localized opacity in the myoplasm, by a 'kink' which remains even after stretching, by localized changes in diameter or by localized contractures. The impaled fibres, judged to be damage-free after prolonged equilibration, showed resting potentials and electrolyte composition comparable to those reported by others (Hagiwara, Chicibu & Naka, 1964; Beaugé & Sjodin, 1967; Brinley, 1968; McLaughlin & Hinke, 1968; Gayton, Allen & Hinke, 1969). Fig. 7 will show, however, that even these carefully selected fibres had resting potentials from -45 to -90 mV.

RESULTS

Uptake of the indicators

The time course of penetration for the extracellular space marker ([^{3}H]inulin) into the single fibre can be expressed as the ratio (V_e/V_t) of the calculated volume of the extracellular space to the total fibre water content (assuming water density is 1 g/cm^3 in both cases). This quantity is suitable for comparison between different fibres. The same calculation can be done for the [^{14}C]DMO marker, to yield a space which has no significance as a volume but which is useful as a cell-specific index for comparison of the DMO content in different fibres.

Ideally, when the uptake of [^{14}C]DMO or [^{3}H]inulin is calculated in this manner and plotted against time of exposure to the isotopes, the resulting curve for each isotope should show a fast initial rise from zero to a value which remains constant with time. Actually, what one finds is a fast initial rise followed by a slow sustained rise which is nearly linear with time. In Fig. 1, for example, are shown the curves for the uptake of [^{14}C]DMO and [^{3}H]inulin by the fibres of one bundle (after the 2 hr preincubation period in non-radioactive normal Ringer) placed at time zero into the normal Ringer solution containing the two isotopes. The slow linear rise in both these curves is usually interpreted as the result of some

non-saturable non-specific adsorption and not as slow entry of the isotopes into regions to which access is difficult. This interpretation is supported by the finding that the addition of 1 mM unlabelled DMO (more than sixty-five times the concentration of [^{14}C]DMO) to the Ringer solution, both before and during uptake, did not produce any change in the

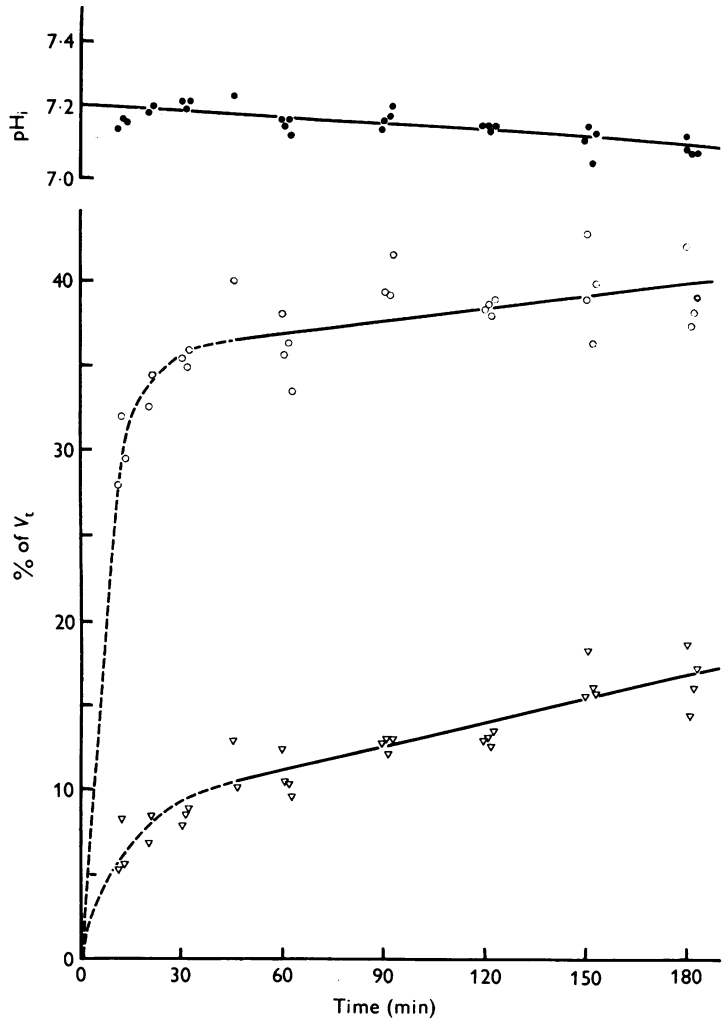

Fig. 1. Uptake of indicator compounds with time by fibres in normal Ringer solution after 2 hr of pre-incubation in non-radioactive Ringer. The data (▽, inulin; ○, DMO) are from one muscle and each datum entry is from one fibre. Continuous lines are plotted from a linear regression and dashed lines are drawn by hand. Also included is a calculated pH_i (●) for each fibre using eqn. (2).

slopes of the 'plateau' of the [^{14}C]DMO or [^{3}H]inulin uptake curves. The slow uptake for [^{14}C]DMO and [^{3}H]-inulin, as in Fig. 1, was rather similar in all ten experiments but an inspection of Figs. 2 and 3 shows that the 'plateau' slopes for [^{14}C]DMO and [^{3}H]inulin can be opposite to one another. This indicates that the adsorption of DMO and inulin are quite independent of one another.

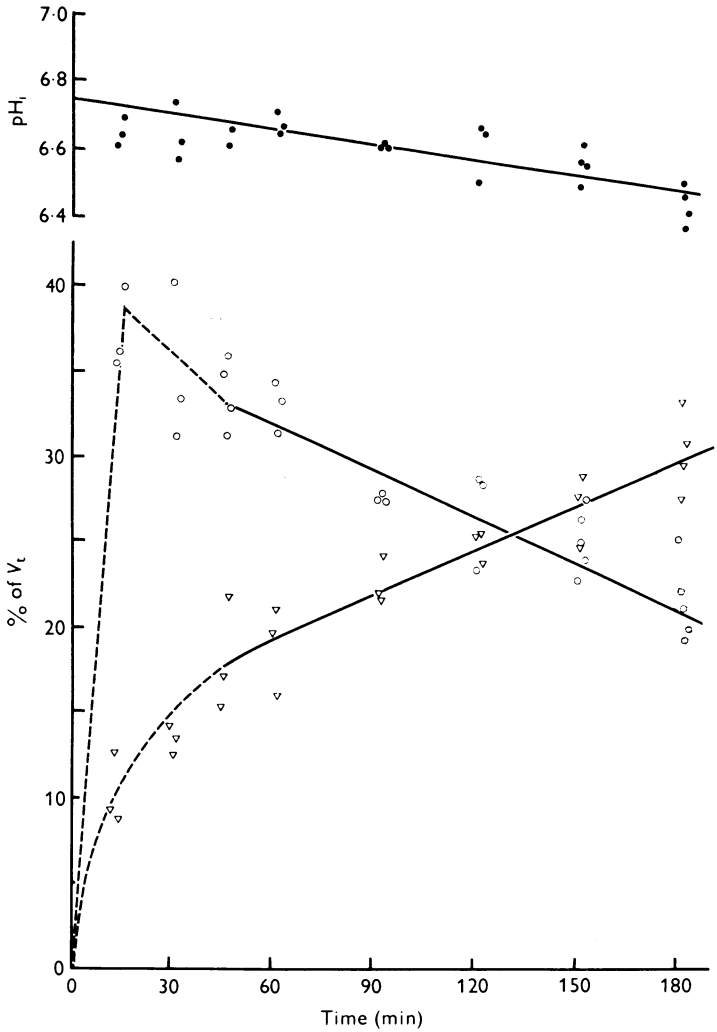

Fig. 2. Uptake of indicator compounds with time by fibres in CO_2 Ringer solution after 2 hr of pre-incubation in non-radioactive CO_2 Ringer. Symbols are as in Fig. 1. Note that all the DMO uptake values (○) were divided by 5·5 to facilitate plotting. Also included is a calculated pH_i (●) for each fibre using eqn. (2).

Intrafibre pH from DMO

The double isotope technique permitted one to calculate a pH(DMO) for every fibre removed from the bath (using eqn. 2). For example, the intrafibre pH(DMO) points in the upper curve of Fig. 1 were obtained from the [^{14}C]DMO and [^{3}H]inulin points of the two uptake curves of the same figure. Notice that all the pH(DMO) values are rather similar, i.e.

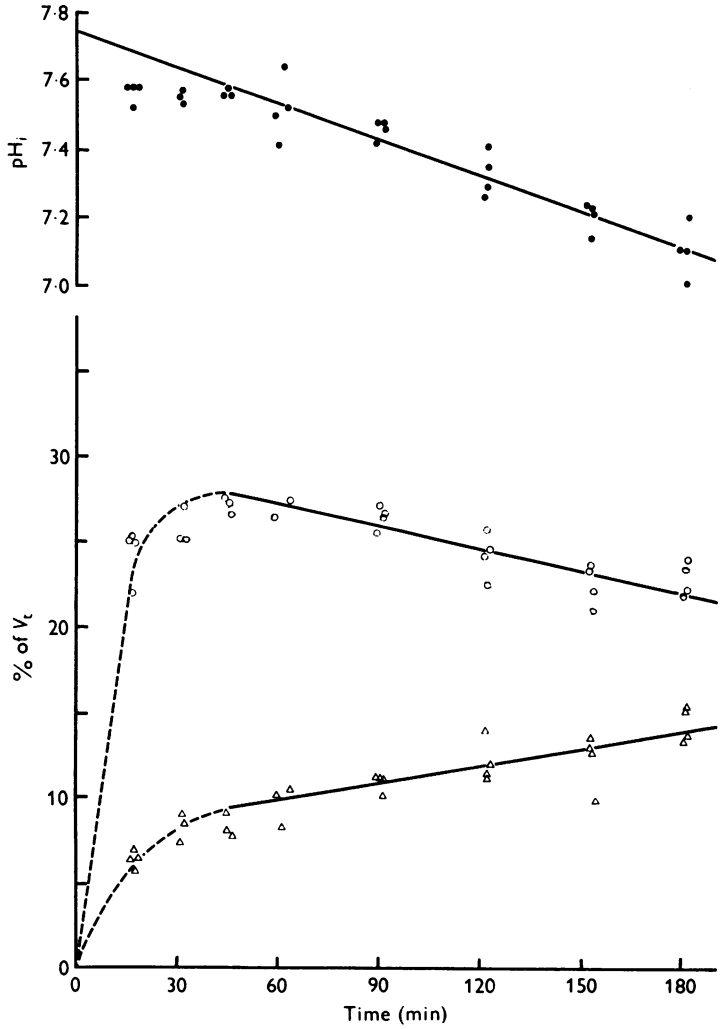

Fig. 3. Uptake of indicator compounds with time by fibres in NH_4^+ Ringer solution after 2 hr of pre-incubation in non-radioactive NH_4^+ Ringer. Symbols are as in Fig. 1. Also included is a calculated pH_i (●) for each fibre using eqn. (2).

they change very little with uptake time. Even during the first 10 min when [^{14}C]DMO and [^{3}H]inulin are taken up rather rapidly, the calculated pH(DMO) is surprisingly similar to the pH(DMO) values for the slow rise period (times greater than 45 min). The bath pH for this experiment remained constant at 7·79.

An example of double isotope uptake during low pH conditions is shown in Fig. 2, and an example during high pH conditions is shown in Fig. 3. For all three conditions (Figs. 1–3), the pH(DMO) curve consistently declined linearly with time and it does not appear to be at all related (at least in an obvious way) to the uptake behaviour of either one of the two isotopes. (See Discussion.)

All the [^{14}C]DMO uptake points in Fig. 2 were divided by a factor of 5·5 in order to present the data of the low pH experiment in a more compact form. The fact that it was necessary to do this illustrates that a great deal more neutral DMO is available for intrafibre penetration under low pH conditions than under normal or high pH bath conditions. For example, the concentration of neutral DMO (pK = 6·17) should increase sixteen times when the bath pH is lowered from 7·66 to 6·20 (Table 1).

TABLE 1. Mean extracellular space of the single fibre from [^{3}H]inulin uptake curves measured by extrapolating the regression line of the 'plateau' (> 45 min) to zero time

Equilibration bath	Bath pH	No. of expts.	Extracellular space % fibre water
Normal Ringer	7·66 ± 0·02*	7	8·23 ± 0·52
CO_2 Ringer	6·20 ± 0·04	6	14·00 ± 1·64
NH_4^+ Ringer	8·23 ± 0·03	2	7·86 ± 0·005

* S.E. of mean.

Intrafibre pH from micro-electrodes

Figs. 4 and 5 provide examples of changes in pH_i, extracellular pH value (pH_o) and E_m with time following impalement by the two micro-electrodes (e.g. Fig. 4) and following a bath change. These tracings were constructed from data taken every 5–15 min (where necessary) from original continuous recordings. In Fig. 4, fibre *A* was allowed to equilibrate for 105 min after impalement. During this period, the internal pH_i was remarkably constant even though the resting potential increased from −75 to −81·5 mV and the external pH_o decreased from 7·69 to 7·62. So called acid injury and slow recovery following electrode penetration as described by Thomas (1974) and Aickin & Thomas (1975) using the recessed-tip pH micro-electrode was not observed by us using the spear-type pH micro-electrode. Following the bath change to CO_2 Ringer,

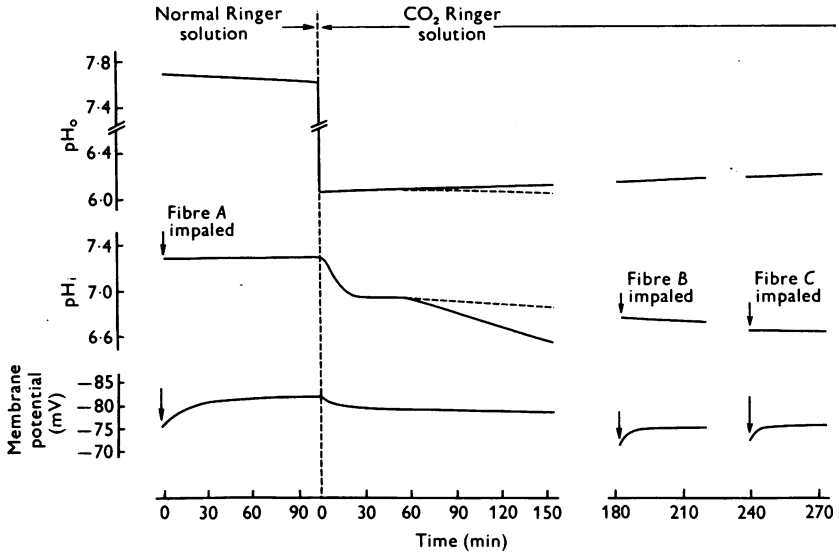

Fig. 4. Re-constructed tracings of pH_i and membrane potential (E_m) from three fibres of a muscle which was subjected to a bath change from normal Ringer to CO_2 Ringer solution. Vertical arrows indicate when each fibre was impaled. pH_o is the extracellular pH value.

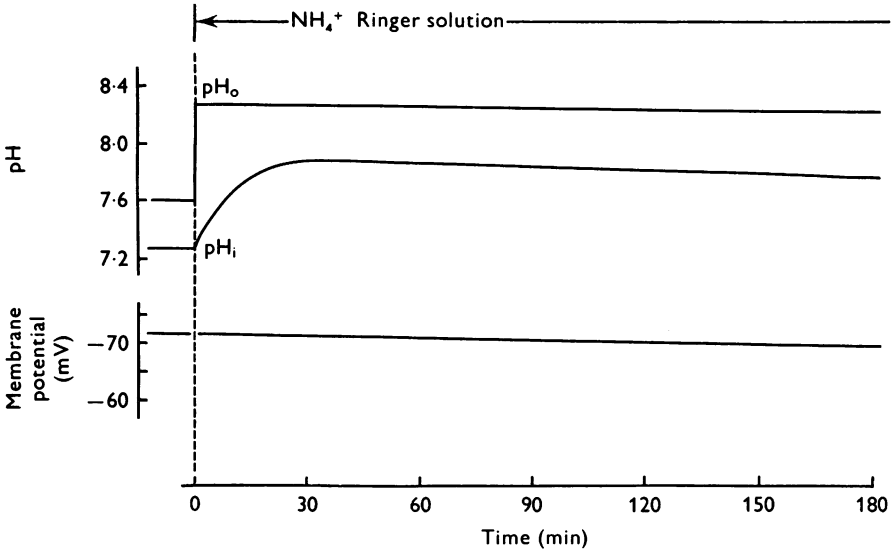

Fig. 5. Re-constructed tracings of pH_i and membrane potential (E_m) from one fibre of a muscle which was subjected to a bath change from normal Ringer to NH_4^+ Ringer solution. Not shown are the complete tracings following electrode impalement which occurred at 90 min before zero time.

the internal pH_i of fibre *A* decreased from 7·31 to 6·94 in 30 min, remained relatively stable for the next 30 min then began to decrease for no apparent reason. Although interesting, such behaviour by a fibre (*A*) was considered undesirable and hence fibres showing it were not used in any analysis either with pH(DMO) (Fig. 6) or with E_m (Fig. 7). To be acceptable for analysis, the pH_i and pH_o tracings would have to follow the dashed lines shown and extend beyond the 120 min mark. Also included in Fig. 4 are recordings from two companion fibres with an identical solution exposure as fibre *A*. Fibre *B* was impaled after 180 min and fibre *C* was impaled after 240 min equilibration in CO_2 Ringer solution. The behaviour of these fibres was considered acceptable, hence the data obtained were used.

Fig. 5 shows a typical partial tracing from a fibre which was allowed to equilibrate for more than 60 min in normal Ringer following electrode impalement (not shown) then exposed to NH_4^+ Ringer for about 200 min. The pH_i, pH_o and E_m values at the 150 min mark were accepted for the Figs. 6 and 7 analyses.

Variation in extracellular space

In Table 1, extracellular space values are listed for the experiments in which [^{3}H]inulin was used as the extracellular marker. Each value was obtained by extrapolation of a regression line through the points after 45 min of a [^{3}H]inulin uptake curve. These data indicate that the extracellular space of fibres bubbled with CO_2 appears to have increased significantly. It should be emphasized, however, that all variations in extracellular space (real or apparent) are accounted for in the pH(DMO) calculation because of the double isotope technique.

Electrolyte and water content of fibres

After several statistical analyses between the Na^+, K^+ or water content of each fibre, on the one hand, and the intrafibre pH or the transmembrane pH gradient, on the other hand, no significant dependencies were uncovered. For this reason, it is sufficient to show only mean values of fibre [Na^+], [K^+] and % water (Table 2) in order to provide an indication of the physiological state of the fibres under the three experimental conditions. Most of the variations demonstrated here are probably due to animal variations (related to size, age, season and nutrition) rather than to experimental conditions, although the relatively high [Na] for fibres bubbled with CO_2 is consistent with the observation that these fibres may have an increase in their extracellular space (Table 1). Note also the marginal increase in % water for the CO_2 bubbled experiment which may also be due to an increase in extracellular space.

Comparison of pH(DMO) and pH_i results

Two methods were adopted to compare the pH(DMO) values with the pH_i values in the three experiments. In one (Fig. 6*A*), the pH(DMO) value at zero time (obtained by extrapolation to zero time of the regression line through the points after 45 min of the pH(DMO) curve) is compared to the mean pH_i for micro-electrode measurements on companion fibres selected as described. In the second method (Fig. 6*B*), the mean of all pH(DMO) values after 45 min is compared to the same mean pH_i. The

TABLE 2. Mean water and electrolyte content of the single fibre* during the three equilibrium conditions

Equilibration bath	No. of fibres	Fibre water (%)	Fibre [Na] (m-mole/kg fibre water)	Fibre [K]
Normal Ringer	73	74·56 ± 0·11†	42·9 ± 1·3	172·4 ± 1·6
CO_2 Ringer	55	75·10 ± 0·15	50·4 ± 2·3	182·3 ± 2·3
NH_4^+ Ringer	16	73·90 ± 0·28	36·6 ± 3·4	181·0 ± 2·1

* Extracellular space included.
† S.E. of mean.

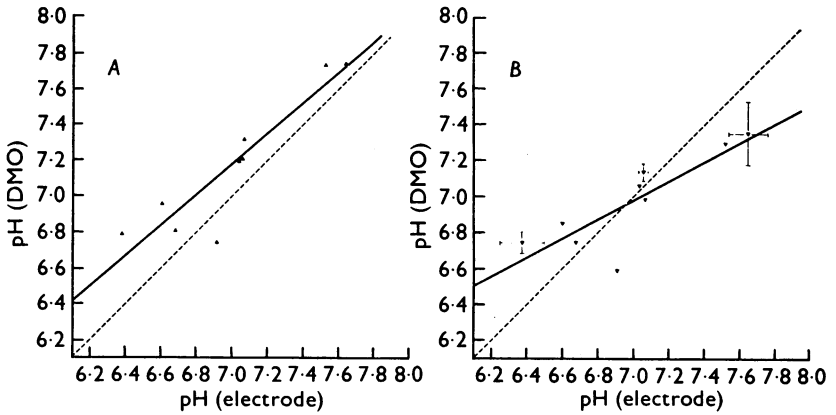

Fig. 6. Calculated value of pH(DMO) plotted versus the mean of values measured with the glass micro-electrode (with inulin as extracellular marker). The dashed line indicates equality. The continuous line is the regression line for the data. *A*, pH(DMO) is calculated by extrapolation to zero time of data taken after 45 min, as explained in the text. *B*, pH(DMO) is calculated as the mean for all cells measured after 45 min, as explained in the text. Bars indicate plus or minus 1 S.D. for five pH (electrode) and for sixteen to twenty-three pH(DMO) measurements.

'extrapolated' pH(DMO) value in Fig. 6*A* should be independent of artifacts due to non-specific adsorption of the two indicators. The second method is similar to the common practice of assuming that DMO uptake reaches a single constant value after 1 hr. Only complete experiments are represented in Fig. 6*A* and 6*B*, i.e. a full double isotope uptake experiment combined with successful micro-electrode impalements of at least three and usually five fibres.

Notice in Fig. 6*A* that the 'extrapolated' pH(DMO) value is nearly always higher than the mean pH_i value. For example, the regression line

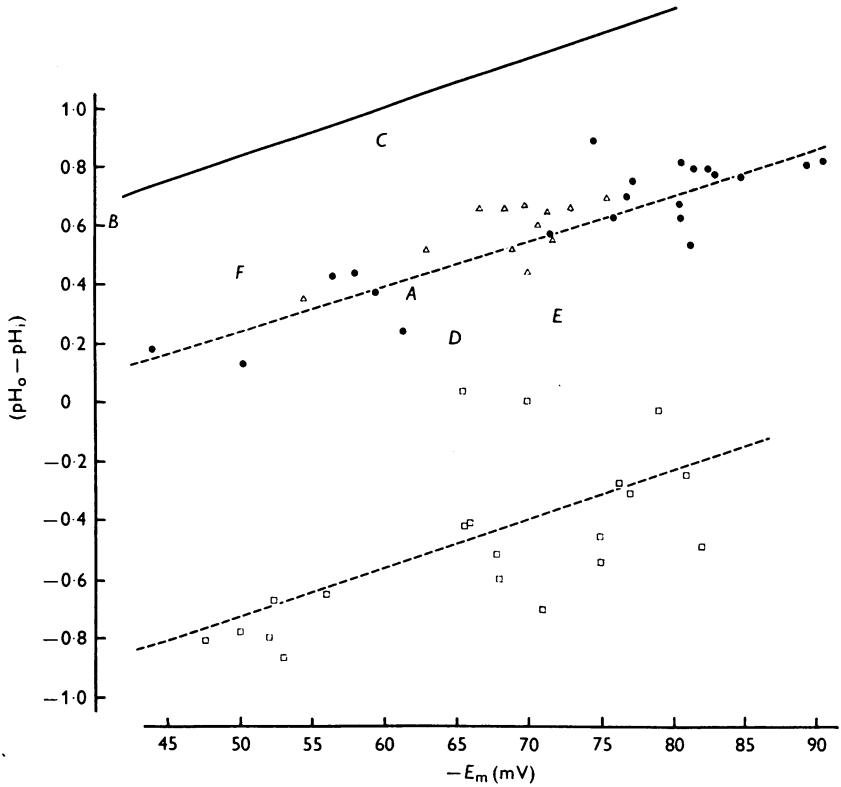

Fig. 7. Relationship between the $\log_{10}$ transmembrane H^+ ion gradient and resting membrane potential from single fibres equilibrated for more than 2 hr in one of three solutions: ●, normal Ringer; △, NH_4^+ Ringer; □, CO_2 Ringer. The two dashed lines are the regression lines for the normal Ringer data (●) and the CO_2 Ringer data (□); the regression line for the NH_4^+ Ringer data (△) is not shown (see Table 3). The upper continuous line represents the Gibbs–Donnan relation. Note that a fibre is only represented once in this plot and no fibre is included if its pH_i was found to vary by more than 0·04 in 30 min after a 2 hr incubation. Fibre membrane potential and bath pH_i always varied less than pH_i. Letters *A*–*F* represent the data in Table 4.

(continuous) through the points predicts a pH(DMO) of 7·18 when pH_i is 7·00. Since the regression line is nearly parallel to the identity line (dashed), one can expect the 'extrapolated' pH(DMO) values to predict correctly the change in intrafibre pH. Observe in Fig. 6*B*, however, that the regression line for the 'plateau' pH(DMO) values crosses and is not parallel to the identity line. It is unlikely, therefore, that measured changes in 'plateau' pH(DMO) would correctly reflect the real changes in intrafibre pH. More will be said on this point later.

TABLE 3. Calculation of the additional flux (j_m) from regression lines in Fig. 7

	Ringer solutions		
	NH_4^+	Normal	CO_2
No. of experiments	12	21	20
pH_o mean	8·18	7·84	6·19
S.E. of mean	±0·007	±0·03	±0·016
$\frac{F}{2{\cdot}3RT}$			
mV^{-1} (slope)	−0·0140	−0·0155	−0·0165
S.E. of mean	±0·004	±0·002	±0·005
y-Intercept*	−0·37	−0·52	−1·55
S.E. of mean	±0·30	±0·14	±0·32
j_m/P_H (mole.cm^{-3} at $E_m = -70$ mV)	$1{\cdot}1 \times 10^{-11}$	$3{\cdot}0 \times 10^{-11}$	$1{\cdot}8 \times 10^{-9}$

* *y*-intercept $= \log_{10}\left[1 - \frac{j_m}{P_H(H)_o}\left(\frac{1-\exp\{FE_m/RT\}}{FE_m/RT}\right)\right]$, where P_H is the passive H^+ permeability and $(H)_o$ is the external H^+ concentration.

pH_i vs. membrane potential

In Fig. 7, the transmembrane H^+ gradient ($pH_o - pH_i$), measured by the pH micro-electrode, is plotted against the corresponding membrane potential (E_m) obtained from conventional micropipettes. This plot only includes fibres which showed no signs of damage after at least 2 hr equilibration in one of the three solutions and revealed a pH_i which did not change by more than 0·04 units in a 30 min recording period. The recorded pH_o and E_m of these selected fibres usually showed less variation than pH_i (e.g. Fig. 5). Only one pH_i and one E_m was taken from a fibre recording. From above downward, the continuous line represents the Gibbs–Donnan relation for hydrogen, $pH_o - pH_i = -(FE_m)/2{\cdot}3RT$, the upper dashed line is a regression line for fibres in normal Ringer and the lower dashed line is a regression line for fibres in CO_2 Ringer. The regression line for fibres in NH_4^+ Ringer is not shown. The statistical slope and *y*-intercept for each regression plot are listed in Table 3. Fig. 7 clearly

shows that the three equilibria do not conform to a Donnan equilibrium for H^+ across the muscle membrane but they do show a dependency on membrane potential with a Donna-type slope ($-zF/RT$).

DISCUSSION

pH_i from DMO uptake

The double isotope uptake data produce reasonable pH_i values for the three experimental equilibrations, but the disturbing feature is that in a given uptake experiment the change in pH(DMO) with time does not relate well to the corresponding changes in [^{14}C]DMO and [^{3}H]inulin uptake. Whether or not the [^{14}C]DMO plateau increased (Fig. 1) or decreased (Figs. 2 and 3), the calculated pH(DMO) consistently declined. Furthermore, the rate of decline in pH(DMO) was usually faster than the rate of decline in pH_i measured by the micro-electrode in a fibre under similar conditions (e.g. compare Fig. 3 pH(DMO) with Fig. 5 pH_i).

The merits and demerits of the weak acid distribution method for determining internal pH_i have been adequately discussed over the years (Fenn & Maurer, 1935; Caldwell, 1956; Waddell & Bates, 1969) and need not be enumerated here. However, faced with the observations from Figs. 1–3 that calculated pH(DMO) appears to be of the correct magnitude but declines consistently relative to electrode pH_i, we decided to re-examine eqn. (2) to see which of its seven parameters if any might dominate. To obtain a rough indication of how a variation in each parameter affects pH(DMO), the partial derivative of pH(DMO) with respect to each parameter was evaluated at a typical point in the 'plateau' region of Fig. 1. For each parameter, X, the change δX required to change pH(DMO) by 0·1 was evaluated from

$$\delta\mathrm{pH(DMO)} = \frac{\partial \mathrm{pH(DMO)}}{\partial X}\,\delta X.$$

This exercise shows that each parameter except pH_o must vary from 5 to 25% to effect a 0·1 change in pH(DMO). The pH_o parameter need only vary by 1%. Admittedly, these calculations provide a crude estimate of pH(DMO) sensitivity per parameter since each partial derivative is itself a function of all other parameters. Nevertheless, the calculations do indicate that observed changes in pH(DMO) as shown in Figs. 1–3 probably do not arise from errors in the measurement of parameters.

No single reason can be extracted from eqn. (2) to explain the apparent stability of pH(DMO) relative to [^{14}C]DMO and [^{3}H]inulin. It is worth pointing out, however, that the argument of the logarithm contains ratios of parameters which tend to change in a similar manner. Specifically, the

partial derivative of pH(DMO) with respect to D_H and D_C are of opposite sign, while both D_H and D_C are increasing initially.

'Plateau' pH(DMO) vs. 'extrapolated' pH(DMO)

A comparison between Fig. 6*A* and *B* indicates that the pH(DMO) from the 'plateau' region, $pH(DMO)_p$, does not correlate with pH_i as well as the 'extrapolated' value $pH(DMO)_e$ does. This finding is best illustrated by an examination of the regression lines:

$$pH(DMO)_p = 0{\cdot}54\ pH_i + 3{\cdot}22 \text{ for the line in Fig. } 6B, \text{ and}$$
$$pH(DMO)_e = 0{\cdot}85\ pH_i + 1{\cdot}22 \text{ for the line in Fig. } 6A,$$

for a pH_i range from 6·4 to 7·7. Boron & Roos (1976) have also measured pH(DMO) and pH_i on barnacle fibres. They measured 'plateau' pH(DMO) and found it to be 7·28 when pH_i was 7·34. At the same pH_i, our Fig. 6*B* regression line gives a 'plateau' pH(DMO) of 7·18.

Since the 'plateau' pH(DMO) value is usually employed by most investigators it is important to assess whether any serious errors can be introduced by its use. Roos (1975), for example, found a good correlation ($r^2 = 0{\cdot}77$) between the transmembrane lactate concentration ratio and the transmembrane H^+ concentration ratio (obtained from 'plateau' pH(DMO) measurement) in the rat diaphragm. If Roos' internal pH(DMO) values are re-calculated according to the regression line in Fig. 6*B* and his Fig. 1 is re-plotted, the result is a poor correlation ($r^2 = 0{\cdot}09$) between lactate and hydrogen ratio rather than a strong correlation. Therefore, it is quite probable that use of 'plateau' pH(DMO) values may lead to erroneous conclusions. This exercise, however, does not necessarily mean that Roos' finding is erroneous since Fig. 6*B* may not be transferrable to the rat diaphragm.

There should, of course, be no difference between the 'plateau' pH(DMO) and the 'extrapolated' pH(DMO) values if the plateaus of both isotope uptake curves are horizontal. We did not find this to be so in any of our uptake curves even when excess non-radioactive DMO was added to the bath. Perhaps, the important advice to investigators wishing to use the DMO method to obtain internal pH is that several points are required beyond the 40 min mark in order to assess the slope of the 'plateau' region. Once several points have been obtained, the investigator might as well calculate a regression line and evaluate pH_i at zero time.

H^+ and Donnan equilibrium

Fig. 7 clearly illustrates that the H^+ ion never reached a Gibbs–Donnan equilibrium across the membrane even in fibres (filled circles) which were exposed from 3 to 5 hr to normal Ringer solution. It is worth emphasizing

again that all the points in Fig. 7 are from fibres which showed no evidence of damage and which produced reasonably stable pH_i and E_m values (as in Fig. 5) after at least 2 hr in the final solution. From these results, one can argue, perhaps with more conviction than before, that the H^+ ion probably never obeys the simple Donnan equation.

Intrafibre pH_i measurements on crustacean fibres with pH glass electrodes have now be done by a number of investigators. Their mean pH_i and E_m values, when the fibre was in normal solutions, are listed in

TABLE 4. Reported mean electrode pH_i and E_m values for crustacean fibres in normal pH_o solutions

Animal type	Mean E_m (mV)	Fibre pH_i	$(pH_o - pH_i)$ Experiment	$(pH_o - pH_i)$ Theory*	Reference
(*A*) *Maia squinado*	−62	7·15	±0·40	+1·03	Caldwell (1958)
(*B*) *Carcinus maenus*	−40	7·20	+0·60	+0·67	Caldwell (1958)
(*C*) *C. maenus*	−60	6·91	+0·90	+1·00	Paillard (1972)
(*D*) *C. maenus*	−65	7·27	+0·23	+1·08	Aickin & Thomas (1975)
(*E*) *Balanus nubilus*	−72	7·32	+0·28	+1·20	McLaughlin & Hinke (1968)
(*F*) *B. nubilis*	−50	7·34	+0·46	+0·83	Boron & Roos (1976)

* Obtained from $60(pH_o - pH_i) = -E_m$.

Table 4. Also included is a comparison between the measured and theoretical transmembrane H^+ gradients $(pH_o - pH_i)$, to illustrate that all authors have more or less observed that the H^+ ion does not follow a Donnan distribution across the membrane. To illustrate the point further and to provide a comparison with our data, we have plotted the Table 4 data as *A* to *F* on Fig. 7. The *B* entry from Caldwell (1958) and the *C* entry from Paillard (1972) are somewhat removed from the other points and rather close to the Donnan line. It could be argued that Caldwell's mean value may not be reliable since fairly large electrodes were used resulting in fibre damage and a lowered membrane potential; Paillard's mean value may not be reliable since he used the Carter-type pH electrode (Carter *et al.* 1967) which was demonstrated by Paillard to lack proper insulation.

$(pH_o - pH_i)$ *vs.* E_m

Considerably more interesting is the observation (Fig. 7) that the $pH_o - pH_i$ values from fibres of a given equilibration show a linear dependence on membrane potential with a slope near $F/2{\cdot}3RT$ (Table 3), the slope of the Donnan line. Both Caldwell (1954, 1958) and Kostyuk & Sorokina (1961) searched for a relation between pH_i and E_m but were

unable to establish one. Carter and co-workers (1967) observed a linear relation between $(pH_o - pH_i)$ and E_m but their relation was different in that all their points followed the Donnan line. Furthermore, Carter reported that whenever the E_m was altered the pH_i changed almost instantaneously to an appropriate value along the Donnan line. Although we did not deliberately attempt to change E_m, our experiments provided numerous examples (e.g. Figs. 4 and 5) to indicate that pH_i and E_m often varied independently of each other on a short time scale. It is worth noting that Aickin & Thomas (1975) observed little change in pH_i when the E_m was increased and decreased for 10 min following modest changes in the external K^+ content.

The fact that the three long-term equilibrations appear to follow three regression lines with rather similar slopes (Table 3) equal to $F/2{\cdot}3RT$ suggests that the H^+ ion does attempt to conform to some sort of an electrochemical equilibrium, although certainly not of the simple Donnan type.

One way to explain Fig. 7 is to postulate that the H^+ ion can cross the membrane through two pathways which are independent of each other. If diffusion through one of the pathways is passive, then the net hydrogen flux (j_p) through it is

$$j_p = P_H \left[\frac{FE_m/RT}{1-\exp\{FE_m/RT\}} \right] [(H_i)\exp\{FE_m/RT\} - (H)_o], \qquad (3)$$

where E_m is the membrane potential, $(H)_i$ and $(H)_o$ are the internal and external H^+ concentrations in mole.cm^{-3}, and P_H is passive H^+ permeability through the path in cm.sec^{-1}.

Under conditions when $(H)_i$ and $(H)_o$ are reasonably constant and if $j_p \neq 0$, then an additional net flux (j_m) through the second path must exist so that $j_m = -j_p$, for example, in the simple case where the two paths are completely independent. Substitution for j_p from eqn. (3) and rearrangement leads to

$$\frac{(H)_i}{(H)_o} = \left[1 - \frac{j_m}{P_H(H)_o} \left(\frac{1-\exp\{FE_m/RT\}}{FE_m/RT} \right) \right] \exp\{-FE_m/RT\}. \qquad (4)$$

When the $\log_{10}$ form of eqn. (4) is examined,

$$pH_o - pH_i = \log_{10}\left[1 - \frac{j_m}{P_H(H)_o} \left(\frac{1-\exp\{FE_m/RT\}}{FE_m/RT} \right) \right] - \frac{F}{2{\cdot}3RT} E_m, \qquad (5)$$

one sees immediately how it might be used to explain the regression lines in Fig. 7 with the slope equal to $F/2{\cdot}3RT$ and the y-intercept equal to the square-bracket term.

Obviously, the square-bracket term in eqn. (5) cannot be expected to be a constant during a given equilibration because it contains E_m (round

brackets) and because j_m/P_H might vary with E_m. Nevertheless, since the slope of the three equilibrations appears to be relatively constant and nearly equal to $F/2{\cdot}3RT$ it follows that the y-intercept of a given equilibration (Fig. 7) must be relatively constant at least for the membrane potential range (45–90 mV) in question. It also follows that j_m/P_H must vary with E_m at about an equal and opposite rate as the round bracket term varies.

None of the above speculation on the relative constancy of the slope and y-intercept for a given equilibration can be used, however, to account for the vertical setting of each equilibration relative to the Donnan line. Certainly, the y-intercepts for the normal Ringer group and for the CO_2 Ringer group are significant departures from zero and the CO_2 y-intercept is significantly different from the normal y-intercept (Table 3). Thus, in terms of eqn. (4), a change in the y-intercept probably signifies a real change in the additional flux (j_m).

In Table 3 we show a j_m/P_H calculation for each equilibration when E_m is -70 mV. If one wishes to accept $P_H = 5 \times 10^{-4}$ cm/sec from Woodbury (1971), j_m can be easily calculated. The main point of this exercise is to show how Fig. 7 can be used not only to support the claim that a H^+ transport system exists but also to provide an estimate of its magnitude under different conditions. For example, our analysis indicates that the so called H^+ transport system is required to function about two orders of magnitude faster when the internal pH of the fibre is reduced from 7·2 to about 6·7 during CO_2 bubbling. Our analysis also shows that the H^+ transport system is not challenged when the internal pH is raised to 7·6 by the addition of NH_4^+.

The authors are grateful to Miss E. Nee and Mr L. Nicol for technical assistance. M. R. Menard is in receipt of a Medical Research Council of Canada Studentship. This work was supported by the Medical Research Council of Canada, grant no. 1039.

REFERENCES

AICKIN, C. C. & THOMAS, R. C. (1975). Micro-electrode measurements of the internal pH of crab muscle fibres. *J. Physiol.* **252**, 803–815.

BEAUGE, L. A. & SJODIN, R. A. (1967). Sodium extrusion by giant muscle fibres from the barnacle. *Nature, Lond.* **215**, 1307–1308.

BORON, W. F. & ROOS, A. (1976). Comparison of microelectrode DMO, and methylamine methods for measuring intracellular pH. *J. gen. Physiol.* (in the Press).

BRINLEY, F. J. JR (1968). Sodium and potassium fluxes in isolated barnacle muscle fibres. *J. gen. Physiol.* **51**, 445–477.

CALDWELL, P. C. (1954). An investigation of the intracellular pH of crab muscle fibres by means of micro-glass and micro-tungsten electrodes. *J. Physiol.* **126**, 169–180.

CALDWELL, P. C. (1956). Intracellular pH. *Int. Rev. Cytol.* **5**, 229–277.

CALDWELL, P. C. (1958). Studies on the internal pH of large muscle and nerve fibres. *J. Physiol.* **142**, 22–62.

CARTER, N. W., RECTOR, F. C., CAMPION, D. S. & SELDIN, D. W. (1967). Measurement of intracellular pH of skeletal muscle with pH-sensitive glass microelectrodes. *J. clin. Invest.* **46**, 920–933.

FENN, W. O. & MAURER, F. W. (1935). The pH of muscle. *Protoplasma* **24**, 337–345.

GAYTON, D. C., ALLEN, R. D. & HINKE, J. A. M. (1969). The intracellular concentration and activity of sodium in giant barnacle muscle fibres. *J. gen. Physiol.* **54**, 433-435.

HAGIWARA, S., CHICHIBU, S. & NAKA, K. I. (1964). The effects of various ions on resting and spike potentials of barnacle muscle fibres. *J. gen. Physiol.* **48**, 163–179.

HINKE, J. A. M. (1969). The construction of pNa and pK microelectrodes for the measurement of a_{Na} and a_K in muscle fibres. In *Experiments in Physiology and Biochemistry*, ed. KERKUT, G. A., pp. 1–25. London: Academic Press.

HOYLE, G., MCNEILL, P. A. & SELVERSTON, A. I. (1973). Ultrastructure of barnacle giant muscle fibres. *J. Cell Biol.* **56**, 74–91.

IZUTSU, K. T. (1972). Intracellular pH, H ion flux and permeability coefficient in bullfrog toe muscle. *J. Physiol.* **221**, 15–27.

KOSTYUK, P. G. & SOROKINA, Z. A. (1961). On the mechanism of hydrogen ion distribution between cell protoplasm and the medium. In *Membrane Transport and Metabolism*, ed. KLEINZELLER, A. & KOTYK, A., pp. 193–203. London: Academic Press.

MCLAUGHLIN, S. G. A. & HINKE, J. A. M. (1966). Sodium and water binding in single striated muscle fibres of the giant barnacle. *Can. Jnl Physiol. & Pharmacol.* **44**, 837-848.

MCLAUGHLIN, S. G. A. & HINKE, J. A. M. (1968). Optical density changes of single muscle fibres in sodium-free solutions. *Can. Jnl Physiol. & Pharmacol.* **46**, 247–260.

MENARD, M. R. & HINKE, J. A. (1976). Behavior of the net hydrogen ion efflux from single muscle fibers under various steady state conditions. *Biophysical J.* **16**, 29a.

MENARD, M. R., NEE, E. & HINKE, J. A. (1975). Evaluation of the method of the distribution of weak electrolytes for determination of intracellular pH. *Proc. Can. Fedn Biol. Socs* **18**, 140.

MOON, R. B. & RICHARDS, J. H. (1973). Determination of intracellular pH by ^{31}P-magnetic resonance. *J. biol. Chem.* **248**, 7276–7278.

PAILLARD, M. (1972). Direct intracellular pH measurement in rat and crab muscle. *J. Physiol.* **223**, 297–319.

ROBINSON, R. A. (1967). Buffer solutions. Operational definitions of pH. In *Handbook of Chemistry and Physics*, ed. WEAST, R. C., pp. D 78–82. Cleveland: CRC Press.

ROOS, A. (1975). Intracellular pH and distribution of weak acids across cell membranes. A study of D- and L-lactate and of DMO in rat diaphragm. *J. Physiol.* **249**, 1–25.

ROSE, I. A. (1968). The state of magnesium in cells as estimated from the adenylate kinase equilibrium. *Proc. natn. Acad. Sci. U.S.A.* **61**, 1079–1086.

THOMAS, R. C. (1974). Intracellular pH of snail neurones measured with a new pH-sensitive glass micro-electrode. *J. Physiol.* **238**, 159–180.

WADDELL, W. J. & BATES, R. G. (1969). Intracellular pH. *Physiol. Rev.* **49**, 285–329.

WADDELL, W. J. & BUTLER, T. C. (1959). Calculation of intracellular pH from the distribution of 5,5-dimethyl-2,4-oxazolidine dione (DMO). Application to skeletal muscle of the dog. *J. clin. Invest.* **38**, 720–729.

WOODBURY, J. W. (1971). Fluxes of H^+ and HCO_3^- across frog skeletal muscle cell membranes. In *Acid–Base and Potassium Homeostasis of the Brain, Alfred Benzon Symposium*, no. 3, ed. SIEJSO, B. K. & SØRENSON, S. C., pp. 270–283. New York: Academic Press.